AIAA JOURNAL
Vol. 32, No. 2, February 1994

Damage Evolution Modeling in Orthotropic Laminated Composites

Yu. A. Dzenis* and S. P. Joshi†
University of Texas at Arlington, Arlington, Texas 76019
and
A. E. Bogdanovich‡
Latvian Academy of Sciences, Riga, Latvia

Composites have inherent scatter in elastic and strength properties. A probabilistic model utilizing random material characteristics to predict damage evolution in orthotropic laminated composites is presented in this paper. The proposed model is based on the division of laminated composites into a statistically large number of mesoelements (mesovolumes). The mesovolume is assumed to be large enough to be structurally homogeneous, and at the same time it has to be comparatively small to satisfy the condition of stochastic homogeneity of stress and strain fields. Three modes of mesovolume failure, i.e., fiber breakage and matrix failure in the transverse direction as well as matrix shear cracking, are taken into account. Damage formation in a ply and in a laminate as a whole for a given plane stress state is calculated from the probabilities of mesovolume failure. These probabilities are directly utilized in reducing ply material constants. A numerical algorithm for damage accumulation and deformation history predictions for orthotropic laminated composites are developed. The behavior of a laminated orthotropic composite is presented as an illustrative example. Analysis of angle-ply Kevlar/epoxy laminates subjected to tension, compression, and shear loading is performed. The effect of scatters in elastic and strength characteristics on damage evolution is shown.

Nomenclature

A_{ij} = laminate stiffnesses
D = dispersion characteristic
$E_1, E_2, G_{12}, \nu_{12}$ = laminate elastic constants
$E_1^k, E_2^k, G_{12}^k, \nu_{12}^k$ = lamina elastic constants
h^k = lamina thicknesses
h_0 = laminate thickness
Q_{ij}^k = lamina stiffnesses in material axes
Q'^k_{ij} = lamina stiffnesses in laminate axes
r_c = laminate cumulative damage function
r_i = $[r_{11}, r_{22}, r_{12}]$, laminate damage functions
r_i^k = $[r_{11}^k, r_{22}^k, r_{12}^k]$, lamina damage functions
S_{ij} = laminate compliances
α^k = lamina orientation angles
ϵ_i = $[\epsilon_{11}, \epsilon_{22}, \epsilon_{12}]$, laminate strains
ϵ_i^k = lamina strains
$\tilde{\epsilon}'_i$ = upper failure bound for ply strains
$\tilde{\epsilon}''_i$ = lower failure bound for ply strains
σ_i = $[\sigma_{11}, \sigma_{22}, \sigma_{12}]$, laminate stresses
σ_i^k = lamina stresses
$\tilde{(\ )}$ = random characteristic
$\bar{(\ )}$ = mean value

Received April 7, 1992; presented as Paper 92-2325 at the AIAA/ASME/ASCE/AHS/ASC 33rd Structures, Structural Dynamics, and Materials Conference, Dallas, TX, April 13-15, 1992; revision received June 7, 1993; accepted for publication July 3, 1993.

*Graduate Student, Center for Composite Materials, Department of Aerospace Engineering. Student Member AIAA.
†Associate Professor, Center for Composite Materials, Department of Aerospace Engineering. Member AIAA.
‡Deputy Director, Engineering and Technology Center, currently Visiting Scholar, North Carolina State University, College of Textiles, Raleigh, NC 27695.

Introduction

POLYMER fiber reinforced composites subjected to loads undergo multiple damage formation on several structural levels that corresponds to their complex structural hierarchy. Matrix cracks in unidirectionally reinforced plies of laminated composites are initiated at the early stage of loading, and their accumulation and evolution have a considerable affect on fiber breakage and delamination growth as well as leading to the final failure of the composite.

A continuum damage mechanics approach was applied to analyze composites in Refs. 1-3. The results had shown that the phenomenological damage evolution law proposed for a composite subjected to a complex in-plane stress field allows a satisfactory description of the deformation of a material up to the final failure under various loading paths. Although damage related parameters of the model can be easily obtained from experiments, the phenomenological approach does not account for all of the observed mechanisms of microdamage formation and evolution in reinforced composites.

Probabilistic modeling in conjunction with fracture micromechanics of composites is a promising approach for the prediction of failure and reliability characteristics of composites. It takes into account inevitable variation in properties of the constituents as well as scatter of composite structural parameters. In Refs. 4 and 5 the probabilistic analysis of composite strength and effective properties was carried out using the Monte Carlo simulation technique. The simulation procedure required extensive computational resources for any new set of structural parameters and properties of the constituents.

An analytical probabilistic approach to the reliability analysis of laminated composites was developed in Refs. 6-8. In these papers, a theory of random scalar and vector field excursions was applied for computing the probability of seldom excursions of a random stress-strain field beyond the limiting surface, confining a multidimensional parallelepiped defined by deterministic[7] or random[8] ultimate strengths. The method was applied to reliability analysis of anisotropic composite shells having a random field of initial imperfections.

The topic of the present paper is the probabilistic modeling of damage evolution in orthotropic laminated composites,

treated as a quasistatic process of damage accumulation in each ply.

Problem Formulation

Consider an orthotropic laminated composite consisting of unidirectionally reinforced laminae with initial stochastic elastic material properties $\tilde{E}_{1_0}^k$, $\tilde{E}_{2_0}^k$, $\tilde{G}_{12_0}^k$, $\tilde{\nu}_{12_0}^k$. Index k denotes the ply number. Laminate lay-up is described by ply orientation angles α^k and ply thicknesses h^k. Load increment applied to a laminate results in random stress-strain field in each ply. Even at very low levels of applied load a nonzero probability of ply failure exists, and damages start to accumulate in the composite. Accumulation of damages causes a reduction in laminate stiffness and a redistribution of stresses between plies.

Assume that in-plane stresses applied to a composite are monotonically increasing functions of a parameter t, $\sigma_i(t) = [\sigma_{11}(t), \sigma_{22}(t), \sigma_{12}(t)]$, with parametric derivatives $\dot{\sigma}_i(t)$. Random deformations of the composite can be then calculated using integral equations

$$\tilde{\epsilon}_i(t) = \int_0^t \tilde{S}_{ij}(\tau)\dot{\sigma}_j(\tau)\, d\tau \tag{1}$$

where $\tilde{S}_{ij}$ are current effective laminate compliances. They depend on the current elastic properties of laminae and composite lay-up.

$$\tilde{S}_{ij}(\tau) = L[\tilde{E}_1^k(\tau), \tilde{E}_2^k(\tau), \tilde{G}_{12}^k(\tau), \tilde{\nu}_{12}^k(\tau), \alpha^k] \tag{2}$$

The current elastic constants of laminae are functions of the initial elastic constants and the current damage functions.

$$\tilde{E}_1^k(\tau), \tilde{E}_2^k(\tau), \tilde{G}_{12}^k(\tau), \tilde{\nu}_{12}^k(\tau) = M[\tilde{E}_{1_0}^k, \tilde{E}_{2_0}^k, \tilde{G}_{12_0}^k, \tilde{\nu}_{12_0}^k, r_i^k(\tau)] \tag{3}$$

Damage functions may be calculated using ply random stress-strain field parameters and some appropriate failure criteria.

$$r_i^k(\tau) = R[\tilde{\epsilon}_i^k(\tau), \tilde{\sigma}_i^k(\tau)] \tag{4}$$

Ply stress-strain field parameters are calculated, in turn, from known composite strains $\tilde{\epsilon}_i$ [Eq. (1)].

$$\tilde{\epsilon}_i^k(\tau) = K[\tilde{\epsilon}_i(\tau), \alpha^k]\tilde{\sigma}_i^k(\tau) = P[\tilde{\epsilon}_i^k(\tau), \tilde{E}_1^k(\tau), \tilde{E}_2^k(\tau), \tilde{G}_{12}^k(\tau), \tilde{\nu}_{12}^k(\tau)] \tag{5}$$

L, M, R, K, and P are stochastic functional operators to be specified. According to this approach, current composite elastic properties and, therefore, composite deformations and damage functions are dependent on loading history. To integrate Eq. (1), we need to calculate the stochastic stress-strain field which depends on the stochastic material properties and the deformation history. The failure criterion [Eq. (4)] should be chosen to obtain damage functions. The stiffness reduction algorithm due to damage accumulation in plies [Eq. (3)] has to be specified.

Random Stress-Strain Field Parameters Calculation

Assume that stochastic elastic characteristics of laminae $\tilde{E}_1^k$, $\tilde{E}_2^k$, $\tilde{G}_{12}^k$, $\tilde{\nu}_{12}^k$ are statistically independent and normally distributed random numbers. They can be described using mathematical mean values $\bar{E}_1^k$, $\bar{E}_2^k$, $\bar{G}_{12}^k$, $\bar{\nu}_{12}^k$ and dispersions $D_{E_1^k}$, $D_{E_2^k}$, $D_{G_{12}^k}$, $D_{\nu_{12}^k}$. The mathematical mean value and dispersion of a function of independent random variables $\tilde{y} = f(\tilde{x}_1, \tilde{x}_2, \ldots, \tilde{x}_n)$ can be calculated as follows:

$$\bar{y} = f(\bar{x}_1, \bar{x}_2, \ldots, \bar{x}_n), \qquad D_y = \sum_{i=1}^{n}\left(\frac{\partial y}{\partial x}\right)^2 D_{x_i} \tag{6}$$

Using Eq. (6) and classical lamination theory[9] and assuming that composite lay-up is symmetric, the parameters (mean values and dispersions) of random fields can be calculated in the following sequence: 1) stiffness coefficients of plies in material axes $\tilde{Q}_{ij}^k[\tilde{E}_{1_0}^k, \tilde{E}_{2_0}^k, \tilde{G}_{12_0}^k, \tilde{\nu}_{12_0}^k]$; 2) stiffness coefficients of plies in laminate axes $\tilde{Q}_{ij}'^k[\tilde{Q}_{ij}^k, \alpha^k]$; 3) laminate effective stiffnesses $\tilde{A}_{ij}[\tilde{Q}_{ij}'^k, h^k]$, compliances $\tilde{S}_{ij}[\tilde{A}_{ij}]$, and apparent constants $\tilde{E}_1^k, \tilde{E}_2^k, \tilde{G}_{12}^k, \tilde{\nu}_{12}^k[\tilde{A}_{ij}]$; 4) laminate strains $\tilde{\epsilon}_i[\tilde{S}_{ij}, \sigma_j]$; and 5) ply strains $\tilde{\epsilon}_i^k[\tilde{\epsilon}_i, \alpha^k]$ and stresses $\tilde{\sigma}_i^k[\tilde{\epsilon}_i^k, \tilde{Q}_{ij}^k]$.

In the case of a damaged composite, current elastic properties of laminae have to be used in step 1 instead of the initial properties, as well as the integral equations for the laminate strains calculation in step 4.

Ply Failure Criteria

The maximum strain criterion is applied to calculate the probability of failure of individual laminae. The ply failure is considered independent of the stacking sequence of the laminate. This is a simplifying assumption. In the case of deterministic failure strains, each ply is assigned limiting failure strains in tension and compression, $\epsilon_i'^k$ and $\epsilon_i''^k$, respectively. These limiting values are the same in magnitude for shear strain. In the case of stochastic failure strains these are normal distributions. Normal distribution instead of Weibull distribution is considered because it is more conservative and the differences between the two distributions are insignificant at low scatter.[10] The probability of $\tilde{\epsilon}_i^k$ to exceed deterministic border $\epsilon_i'^k$ is simply the area under differential distribution of $\tilde{\epsilon}_i^k$ on the right side of the upper bound $\epsilon_i'^k$ (see Fig. 1), and can be calculated from integral distribution $F_{\epsilon_i^k}$ of ply strain by using Eq. (7).

$$r_i^k = 1 - F_{\epsilon_i^k}(\epsilon_i'^k) \tag{7}$$

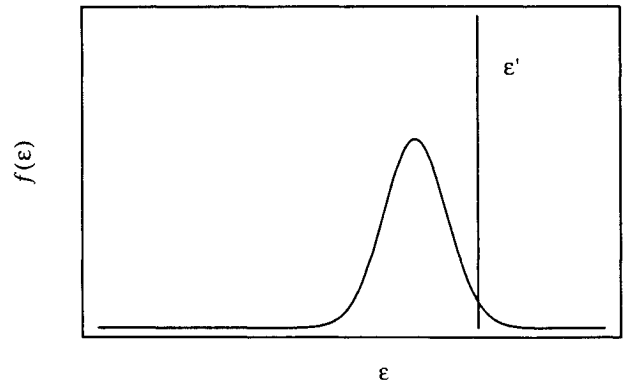

Fig. 1 Schematic representation of normal distribution of strain and deterministic failure strain bound.

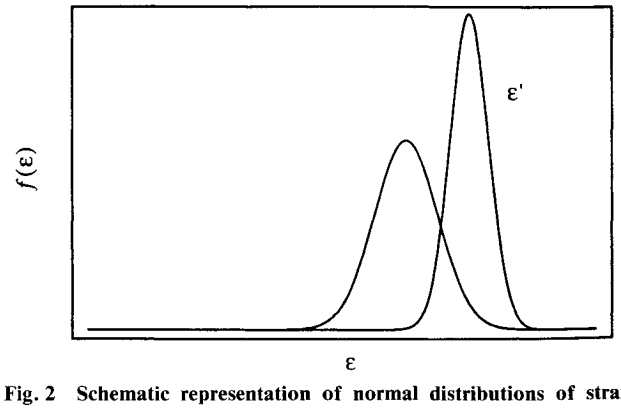

Fig. 2 Schematic representation of normal distributions of strain and failure strain.

For stochastic failure strains $\tilde{\epsilon}_i'^k$ (see Fig. 2), the probability that $\tilde{\epsilon}_i^k$ will exceed $\tilde{\epsilon}_i'^k$ can be calculated as the probability of random difference $\epsilon_i'^k - \tilde{\epsilon}_i^k$ to be negative.

$$r_i^k = F_{\epsilon_i^k - \epsilon_i'^k}(0) \tag{8}$$

Parameters of the integral distribution $F_{\epsilon_i'^k - \epsilon_i^k}$ can be calculated as

$$\begin{aligned} \overline{\epsilon_i'^k - \epsilon_i^k} &= \bar{\epsilon}_i'^k - \bar{\epsilon}_i^k \\ D_{\epsilon_i'^k - \epsilon_i^k} &= D_{\epsilon_i'^k} + D_{\epsilon_i^k} \end{aligned} \tag{9}$$

Taking into account both upper and lower bounds, $\epsilon_i'^k$ and $\epsilon_i''^k$, and assuming that strain field excursions beyond the two bounds are statistically independent events, the following expressions for r_i^k can be derived:

1) Deterministic bounds $\epsilon_i'^k$, $\epsilon_i''^k$

$$r_i^k = 1 - F_{\epsilon_i^k}(\epsilon_i'^k) + F_{\epsilon_i^k}(\epsilon_i''^k) \tag{10}$$

2) Random bounds $\tilde{\epsilon}_i'^k$, $\epsilon_i''^k$

$$r_i^k = F_{\epsilon_i'^k - \epsilon_i^k}(0) + F_{\epsilon_i^k - \epsilon_i''^k}(0) \tag{11}$$

It is easy to show that the second case is reduced to the first case when $D_{\epsilon_i'^k} = D_{\epsilon_i''^k} = 0$.

Effect of Damage on Ply Stiffness

To use the information about failure probability we need to specify how it is realized in the composite, i.e., when and how much damage of different types emerge and how the damages effect the current mechanical properties of the composite. Assume that there are three types of damages related to three in-plane deformations in each ply $\epsilon_i^k = [\epsilon_{11}^k, \epsilon_{22}^k, \epsilon_{12}^k]$. Failure type due to ϵ_{11}^k exceeding the critical bound can be associated with fiber breakage, and failures due to ϵ_{22}^k and ϵ_{12}^k can be associated with matrix cracking in transverse to fiber direction and in shear, respectively.

Assume that each ply consists of a certain number of mesovolumes, structurally homogeneous, i.e., containing a sufficient amount of reinforcing fibers, and comparatively small to satisfy the condition of stochastic homogeneity of stress and strain fields. Initial random characteristics of plies are equal to respective mesovolumes characteristics. Assume that each of the mesovolumes can be either perfect or broken in the fiber direction or/and in the transverse direction or/and in shear. Therefore, at every current state of loading, the relative numbers of broken mesovolumes in plies for each type of failure are proportional to the probabilities of failure r_i^k. In the limiting case of the infinite number of mesovolumes in ply, the proportionality becomes equality. Thus, we can interpret the numbers $r_i^k = [r_{11}^k, r_{22}^k, r_{12}^k]$ as relative counts of broken mesoelements of three failure modes in each ply.

The accumulation of damages in composite laminae causes an apparent stiffness reduction of laminate and stress redistribution around the microcracks and between the plies. This process is very complicated and modeling damage accumulation using microlevel consideration, in general, is not amenable to analytical studies. The probabilistic imitation approach[4] has led to a certain success in the area but it is computationally extensive and needs many simplifying assumptions.

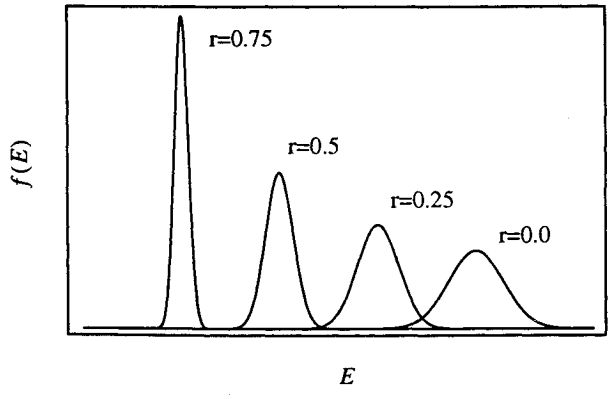

Fig. 3 Schematic representation of stiffness distributions at various damage levels.

It is assumed in this paper that mesoelement failure in a certain direction causes deterioration of properties in the same direction. Failure of the r_i^k fraction of all mesoelements in the ith direction of the kth ply will result in the reduction of ply elastic modulus in this direction. It is proposed that the mathematical mean values of ply elastic moduli decrease with damage accumulation according to the following hypothesis:

$$\begin{aligned} \bar{E}_1^k(\tau) &= \bar{E}_{1_0}^k[1 - r_{11}^k(\tau)] \\ \bar{E}_2^k(\tau) &= \bar{E}_{2_0}^k[1 - r_{22}^k(\tau)] \\ \bar{G}_{12}^k(\tau) &= \bar{G}_{12_0}^k[1 - r_{12}^k(\tau)] \\ \bar{\nu}_{12}^k(\tau) &= \bar{\nu}_{12_0}^k[1 - r_{11}^k(\tau)] \end{aligned} \tag{12}$$

but relative standard deviations remain constant

$$\begin{aligned} \frac{\sqrt{D_{E_1^k(\tau)}}}{\bar{E}_1^k(\tau)} &= \frac{\sqrt{D_{E_{1_0}^k}}}{\bar{E}_{1_0}^k} \\ \frac{\sqrt{D_{E_2^k(\tau)}}}{\bar{E}_2^k(\tau)} &= \frac{\sqrt{D_{E_{2_0}^k}}}{\bar{E}_{2_0}^k} \\ \frac{\sqrt{D_{G_{12}^k(\tau)}}}{\bar{G}_{12}^k(\tau)} &= \frac{\sqrt{D_{G_{12_0}^k}}}{\bar{G}_{12_0}^k} \\ \frac{\sqrt{D_{\nu_{12}^k(\tau)}}}{\bar{\nu}_{12}^k(\tau)} &= \frac{\sqrt{D_{\nu_{12_0}^k}}}{\bar{\nu}_{12_0}^k} \end{aligned} \tag{13}$$

According to this algorithm, damage accumulation in the ply, during laminate loading, evokes the shift of ply moduli distributions toward the zero direction and narrows these distributions proportionally to decreased stiffness. Changes in statistical distributions of stiffness resulting from damage accumulation according to the proposed algorithm of stiffness reduction are illustrated in Fig. 3.

This simple approach does not take into consideration micromechanical phenomena like stress redistribution around single cracks or cracks interaction, but does take into account gradual stiffness reduction due to damage accumulation in plies and stress redistribution between them.

Algorithmic Development

A computer code is developed for calculating the response of orthotropic laminated composites using the described approach. Incremental loading is set in the program according to given parametric derivatives $\dot{\sigma}_i$ and Eq. (1) is integrated numerically. On each step of loading, the damage functions r_i^k accumulated up to the previous step are used to calculate the current elastic properties of material and laminate strain increments. It is assumed that complete failure of the composite occurs when any of the current effective elastic moduli of composite $\bar{E}_1$, $\bar{E}_2$, $\bar{G}_{12}$ becomes equal to zero (in computer code: equal to small number). The program is written in "Mathematica" language.

Composite stiffness reduction during a load increment is implemented by an iterative procedure. Damage functions are iteratively calculated and used for calculating deformations at the same load step until the damage functions do not change during two subsequent iterations. However, it is realized that for sufficiently small load increments an iterative procedure is unnecessary. The results presented in this paper are obtained

without employing an iterative procedure. Sufficiently small load increments were chosen in the calculations.

Numerical Results

The basic feature of the proposed method is the consideration of the stochastic nature of stress and strain fields in the laminate due to stochastic stiffness and strength properties of laminate constituents. In addition, the concept of mesovolume as a building element for laminated composites is introduced. Stochastic characteristics of mesovolumes should be known to perform the analysis. They can be obtained experimentally using small specimens or can be calculated using some appropriate micromechanical models. Experimental statistical data for Kevlar/epoxy unidirectional composite presented in Ref. 11 are used for the mesovolume material properties definition. It is assumed that mesovolumes are linearly elastic until the failure. However, inelastic behavior of mesovolumes can be easily incorporated in the algorithm. The random elastic and strength (critical strain bounds) characteristics are listed in Table 1. The standard deviations of the random characteristics were calculated from their 95% confidential intervals given in Ref. 11, using well-known statistical formulas. Note that the mesovolume concept assumes that the mesoelements are much smaller than the laminate in size. There are statistically large numbers of mesoelements in each ply so that the probability of failure can result in failure of a proportional number of mesoelements. Use of experimental data from Ref. 11 to obtain the mesovolume properties dictates that the following analysis is valid for larger laminates than experimental specimens. If the laminated composite is about the same size as the unidirectional samples, data reduction should be performed to obtain mesovolume properties. Data reduction procedures are beyond the scope of this paper.

The capability of the method is illustrated by considering an example of a Kevlar/epoxy laminate. Laminate lay-up is $[90/60/-60/0]_s$. A complex, linearly increasing load was applied with parametric derivatives $\dot{\sigma}_i(t) = [5t, 10t, 2t]$ MPa (Fig. 4). Continuous lines, dashed lines, and dash-dot lines in the following figures correspond to 11, 22, and 12 variables in laminate coordinate axes, respectively. Calculated composite strains are plotted in Fig. 5 as functions of the loading parameter t. Damage functions $r_i^k = [r_{11}^k, r_{22}^k, r_{12}^k]$ for each ply are shown in Fig. 6. Damage is assumed to be identical in symmetric plies. In Fig. 7, the average content of damages of different types in the laminate

$$r_i = \left[\sum_{k=1}^{n} r_i^k\right]/n$$

is shown and the cumulative damage function of a laminate as a whole

$$r_c = \left[\sum_{i=1}^{3} r_i\right]/3$$

is plotted in Fig. 8.

Damages of different types appear long before the final composite failure of the laminate in the analyzed loading case.

Table 1 Material properties for the Kevlar/epoxy lamina[11]

Characteristic	Average value	Standard deviation	Relative standard deviation, %
E_1, GPa	74.9	2.22	2.97
E_2, GPa	4.65	0.16	3.44
G_{12}, GPa	1.877	0.033	1.76
ν_{12}	0.35	0.031	8.86
ϵ'_{11}	0.0171	0.002	11.7
ϵ''_{11}	−0.00478	0.00024	5.2
ϵ'_{22}	0.00283	0.00016	5.6
ϵ''_{22}	−0.0141	0.0011	7.8
ϵ'_{12}, ϵ''_{12}	±0.0256	0.0079	30.8

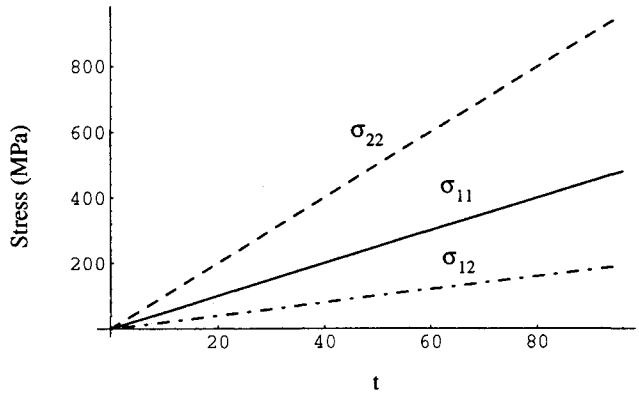

Fig. 4 Applied stresses as functions of loading parameter.

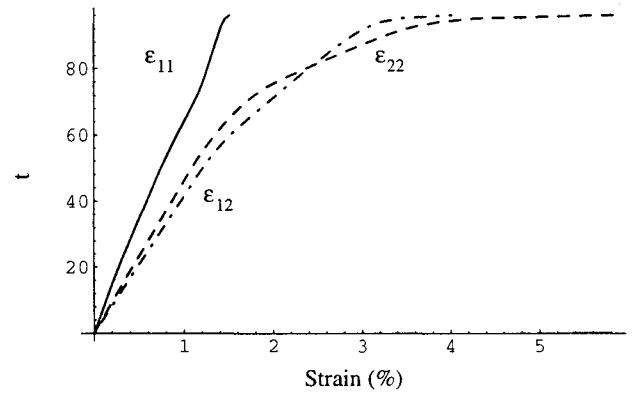

Fig. 5 Deformation behavior of $[90/60/-60/0]_s$ laminate.

First, at a very low load, about 10-20% of the final strength, matrix transverse tension cracks occur in 90, −60, and 0 plies (Figs. 6 and 7). Note that a positive (in tension) bound of mesovolume strain in the transverse to fiber direction is very small (see Table 1). At load levels of about 50 and 65% of final strength, fiber breakage in plies 60 and 90 occurs due to tension, respectively. Starting approximately from 40% of strength, matrix damages in shear are accumulated in 90, −60, and 0 plies. Finally, the laminate breaks after the fiber damages in −60 ply. The cumulative damage function in Fig. 8 shows that the final failure starts to develop rapidly only after about 75% of all of the possible damages in the plies are accumulated. Apparent stiffening of the composite in the zero direction after about 1% deformation (Fig. 5) is due to the Poisson's contraction in this direction because of the laminate intensive stretching in the transverse direction. Current effective laminate elastic moduli (Fig. 9) show the deterioration of laminate properties under loading. Note that the observed apparent stiffening of the material is a direct consequence of the damage accumulation in the laminate.

Figures 10 and 11 show the average damage accumulation for the laminate when the calculations are carried out by using deterministic strain bounds of mesovolumes instead of stochastic bounds. Comparison of Figs. 7 and 10 and Figs. 8 and 11 indicates a late start and the abrupt character of damage accumulation process in the latter case. Analysis for different lay-ups and loads showed a considerable effect of scatters in mesovolumes characteristics on laminate deformation and damage accumulation. The remaining examples presented in this paper are for stochastic failure bounds.

Stress-strain diagrams for Kevlar/epoxy angle-ply laminates subjected to tensile loading are shown in Fig. 12. The laminate lay-up is $[+\alpha, -\alpha]_s$ with α being equal to 15, 30, 45, 60, and 75 deg, respectively. Damage functions for different types of damages are shown in Fig. 13. Note that plies with opposite orientation behave identically in angle-ply laminates under

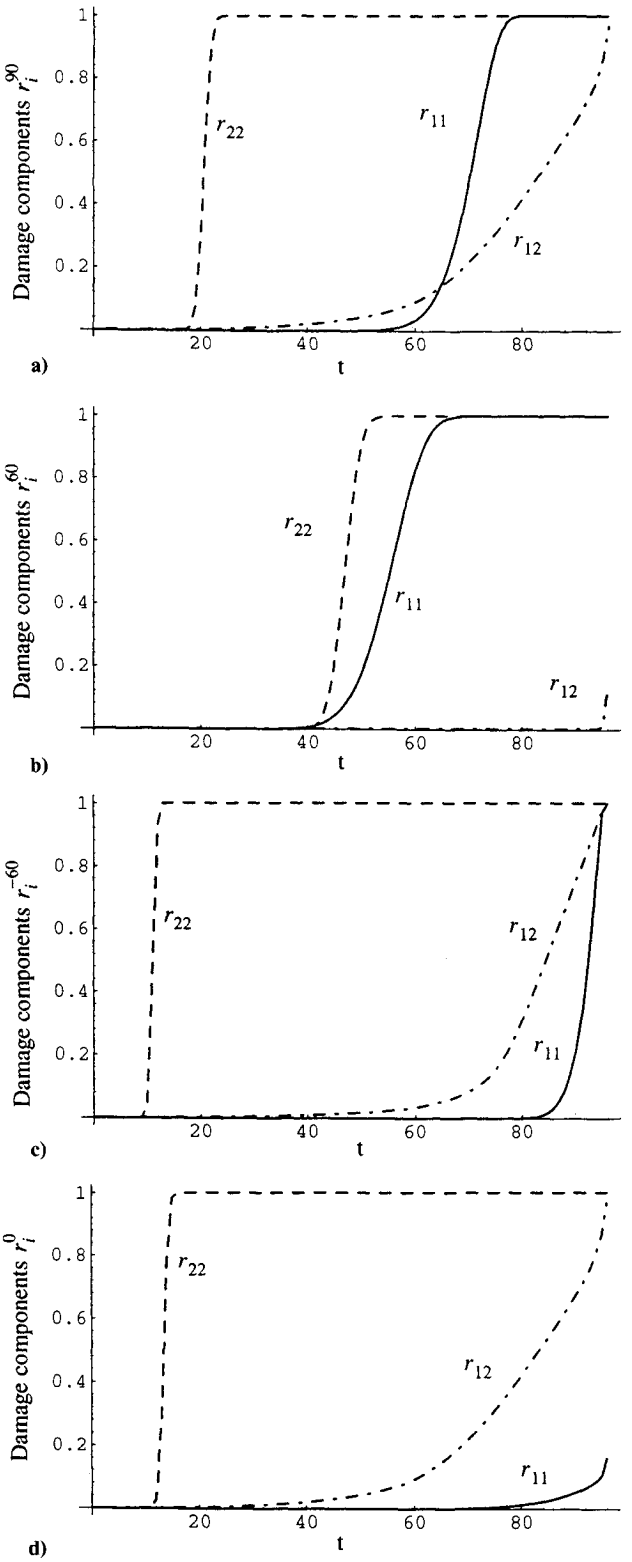

Fig. 6 Damage formation in plies of $[90/60/-60/0]_s$ laminate: a) 90, b) 60, c) −60, and d) 0.

tension-compression loading. The only difference between them is the opposite sign of shear stresses and strains. Cumulative damage parameter r_c for each angle-ply laminate is plotted in Fig. 14.

As was expected, the strength of the laminates in tension gradually decreases with the increase of orientation (Fig. 12), but ultimate failure strain increases only up to about 60-deg fiber orientation. In 15-, 60-, and 75-deg angle-ply laminates, the first matrix cracks appear in the transverse to fiber directions of the laminae (Fig. 13b). For the 15-deg fiber orienta-

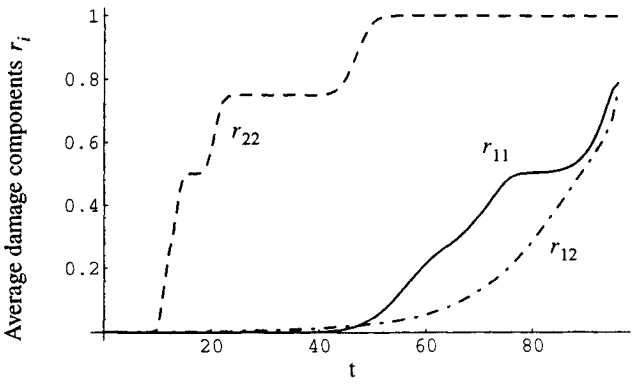

Fig. 7 Average damage formation for $[90/60/-60/0]_s$ laminate.

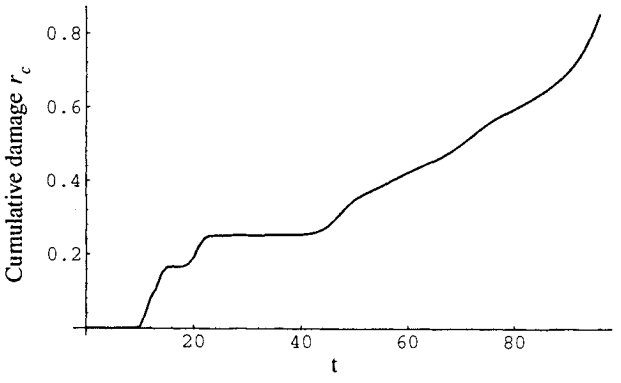

Fig. 8 Total average damage formation in the laminate.

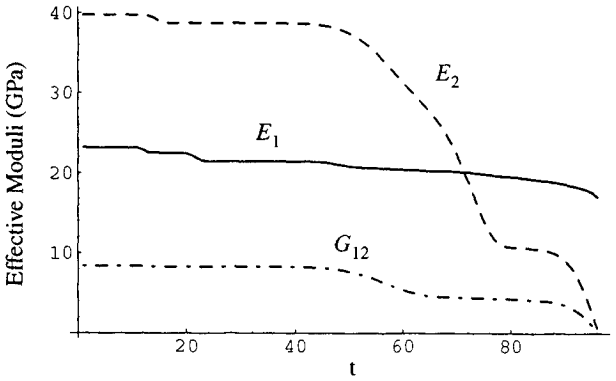

Fig. 9 Reduction in effective moduli of the laminate due to the damage accumulation.

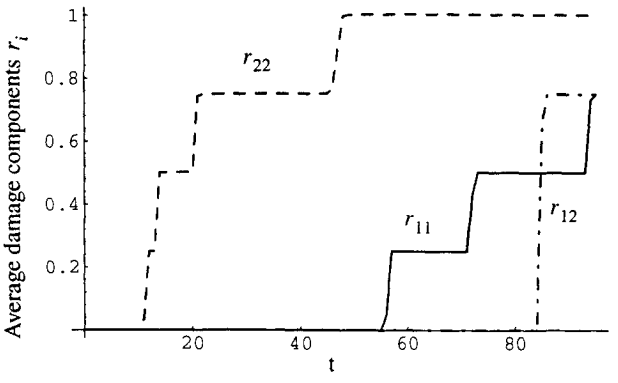

Fig. 10 Average damage formation for $[90/60/-60/0]_s$ laminate using deterministic failure strain bounds.

tion, this cracking is due to compressive strains in the plies, but for the 60- and 75-deg fiber orientations, it is due to tensile strains. Gradual matrix cracking in shear is observed for angle-ply laminates with fiber orientations of 30, 45, and 60 deg, but almost no shear damage occurs in 15- and 75-deg angle-ply laminates. It is interesting to note that only two of the laminates analyzed have a small amount of fiber damage appearing just before the ultimate failure, namely, 15- and 45-deg angle-ply laminates. Other laminates develop no fiber breakage up to the ultimate failure. Angle-ply laminates with 30- and 60-deg orientations have a large damage content at failure (Fig. 14) due to both shear and tensile failure accumulation in the matrix. Figure 15 shows stress-strain behavior of angle-ply laminates under compressive loading. The total average damage accumulation under compressive loading is shown in Fig. 16.

Results of shear analysis of angle-ply laminates are plotted in Figs. 17 and 18. Angle-ply laminates with angles of ply orientation symmetric to about 45 deg have the same response in shear, so only data for the 15-, 30-, and 45-deg laminates are shown, together with the unidirectional composite data. Unlike longitudinal loading, plies with different orientation in angle-ply laminates have distinct damage parameters under shear loads. Figure 18 shows that all angle-ply laminates under shear have high ultimate damage contents due to at least two different kinds of damage accumulation in the laminas. In each laminate analyzed, first a matrix transverse cracking occurs in the ply with a negative angle of orientation (due to tension) and then fiber breakage takes place in the same ply due to compression. Matrix and fiber damage in the ply with positive fiber orientation occur subsequently. The amount of shear matrix cracks rapidly decreases with the increase of fiber

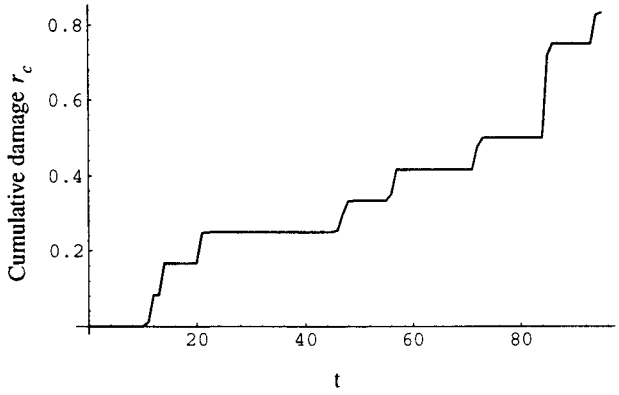

Fig. 11 Total average damage formation in the laminate using deterministic failure strain bounds.

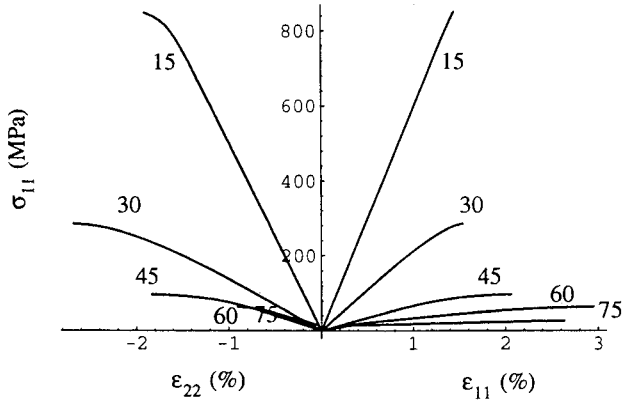

Fig. 12 Stress-strain plots for angle-ply laminates under tensile loading.

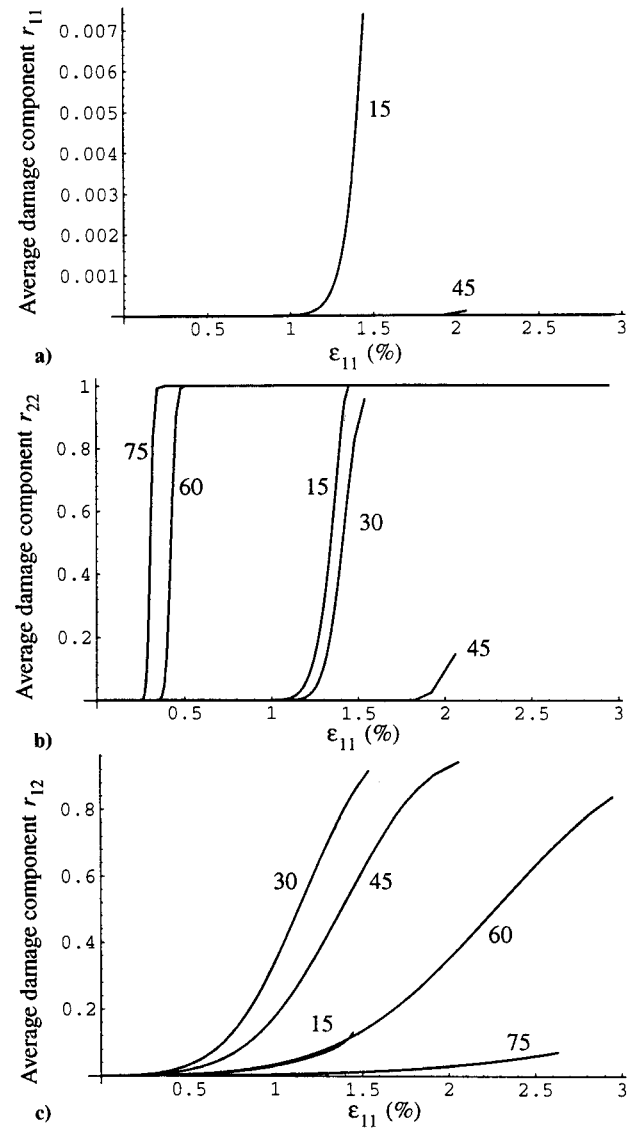

Fig. 13 Average damage formation in angle-ply laminates: a) longitudinal, b) transverse, and c) shear.

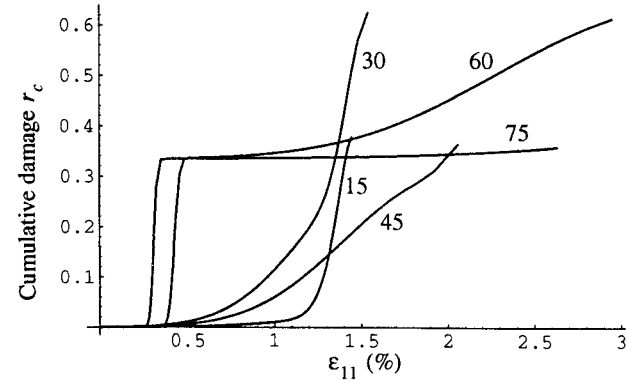

Fig. 14 Total average damage formation in angle-ply laminates subjected to tensile load.

orientation from 0 to 30 deg. The shear damage is practically nonexistent for the 45-deg laminate.

Since experimental results are not available for Kevelar/epoxy composite laminates analyzed in this paper, a direct comparison between theory and observed behavior is not possible. However, the experimentally observed behavior of angle-ply laminates of other composites is characteristically similar to the one presented in this paper (see Ref. 12). Staab and Gilat[13] recently investigated the effect of the strain rate on the behavior of Scotchply type 1002 glass/epoxy in an angle-ply

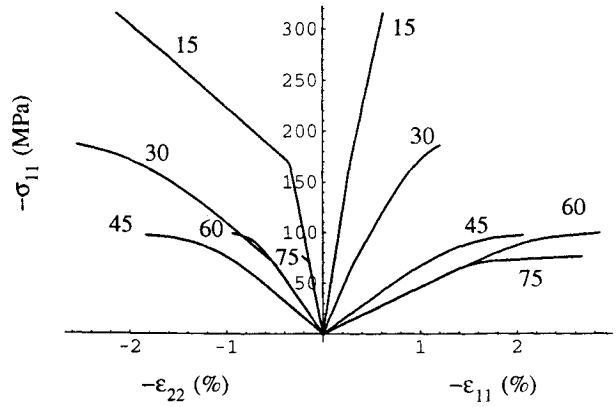

Fig. 15 Stress-strain plots for angle-ply laminates under compressive loading.

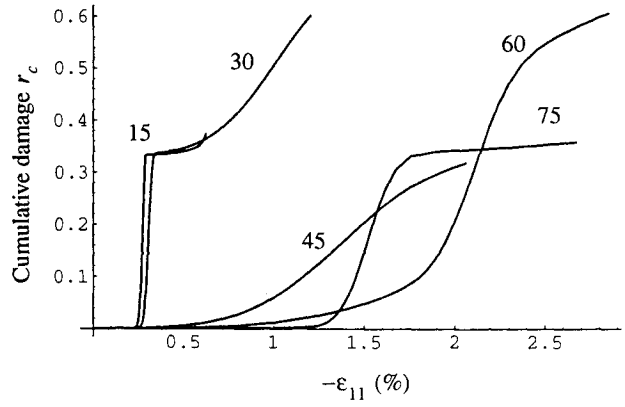

Fig. 16 Total average damage formation in angle-ply laminates subjected to compressive load.

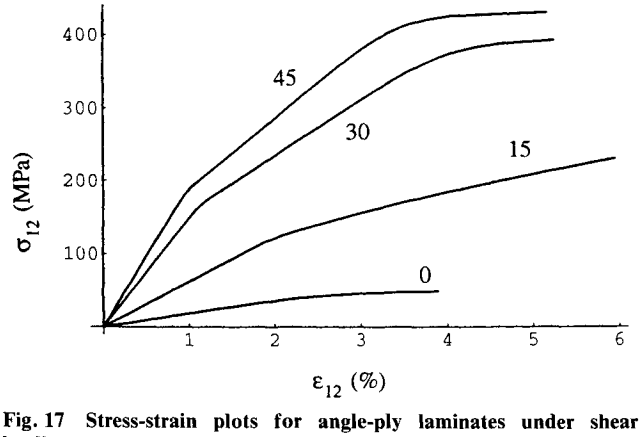

Fig. 17 Stress-strain plots for angle-ply laminates under shear loading.

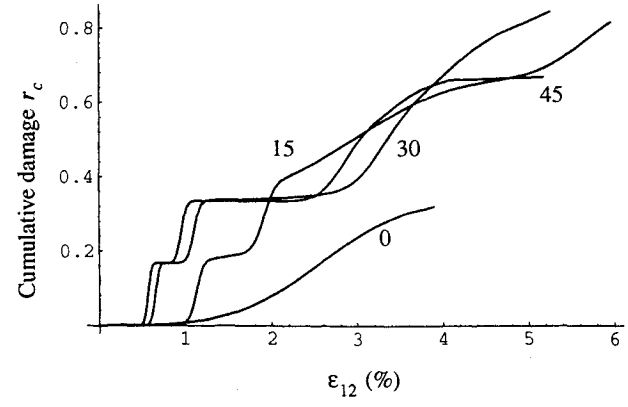

Fig. 18 Total average damage formation in angle-ply laminates subjected to shear load.

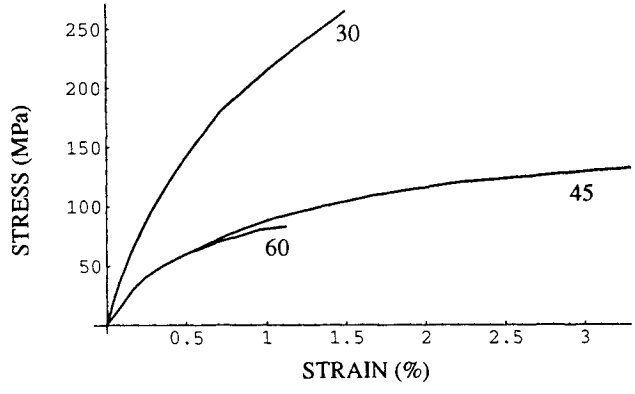

Fig. 19 Experimental stress-strain relations for Scotchply 1002 glass/epoxy angle-ply laminates (Staab and Gilat[13]).

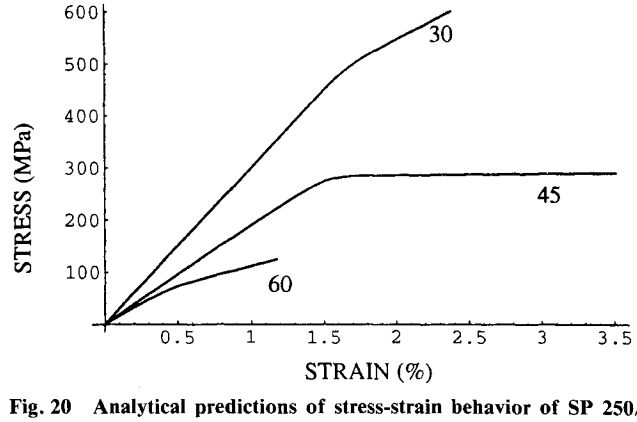

Fig. 20 Analytical predictions of stress-strain behavior of SP 250/S-2 glass/epoxy angle-ply laminate.

configuration. Tests have been conducted at strain rates of approximately 10^{-5} 1/s and 10^{3} 1/s. The stochastic material property data are not avaliable for the material used in the experimental investigation. Some of the material properties of SP250/S-2 are close to a Scotchply type 1002 glass/epoxy composite. Use of these material properties in the analysis allows a qualitative comparision of predictions with experimental observations. The material property information for SP250/S-2 glass/epoxy composite necessary for the analysis are given in Table 2.

Figures 19 and 20 compare the experimentally observed stress-strain behavior for quasistatic loading with the analytically predicted behavior for ± 30, ± 45, and ± 60 angle-ply laminates. Analytical predictions show the same trend as the experimental observations. The quantitative difference may be due to the difference in stiffness and strength properties of

Table 2 Material properties for SP 250/S-2 glass/epoxy and available properties for Scotchply type 1002 glass/epoxy in parentheses

Characteristic	Average value	Standard deviation	Relative standard deviation, %
E_1, GPa	49.4 (39.3)	0.48	0.98
E_2, GPa	16.3 (9.7)	0.34	2.11
G_{12}, GPa	6.35	0.33	5.21
ν_{12}	0.28	0.01	3.57
ϵ'_{11}	0.0318 (0.0246)	0.0018	5.66
ϵ''_{11}	−0.0222 (−0.0224)	0.0006	2.7
ϵ'_{22}	0.003 (0.0021)	0.0009	30.
ϵ''_{22}	−0.0286 (−0.02)	0.0068	23.8
ϵ'_{12}, ϵ''_{12}	±0.0219	0.00149	6.8

Scotchply type 1002 and SP250/S-2 glass/epoxy materials. Table 2 shows the available material properties of Scotchply type 1002 glass/epoxy in brackets for comparison. The average failure strains are calculated from the available failure stresses assuming a linear behavior up to failure in the material directions.

Conclusions

A probabilistic model utilizing random material characteristics to predict damage evolution in orthotropic laminated composites is presented. A numerical algorithm for damage accumulation and deformation history predictions for orthotropic laminated composites is developed. Behavior of a laminated orthotropic composite is presented as an illustrative example. Analysis of angle-ply Kevlar/epoxy laminates subjected to tension, compression, and shear loading is performed. The effect of scatters in elastic and strength characteristics on damage evolution is shown.

Acknowledgment

This work is funded by the Army Research Office. The project monitor is G. L. Anderson.

References

[1]Frantziskonis, G., and Joshi, S. P., "Damage Evolution and Constitutive Behavior of Advanced Composites" *Composite Structures International Journal*, Vol. 16, 1990, pp. 341–357.

[2]Joshi, S. P., and Frantziskonis, G., "Damage Evolution in Laminated Advanced Composites," *Composite Structures International Journal*, Vol. 17, No. 2, 1991, pp. 127–139.

[3]Joshi, S. P., "Two Phase Continuum Damage Mechanics: Application to Brittle Matrix Composites," *Proceedings of International Symposium BMC-3*, Warsaw, Poland, Sept. 1991.

[4]Ovchinskii, A. S., "Fracture Processes in Composite Materials: Computer Imitation of Micro- and Macromechanisms," Nauka, Moscow, 1988, (in Russian).

[5]Stock, T. A., Bellini, P. X., Murthy, L. N., and Chamis, C. C., "Probabilistic Composite Micromechanics," *Proceedings of the AIAA/ASME/ASCE/AHS/ASC 29th Structures, Structural Dynamics, and Materials Conference* (Williamsburg, VA), AIAA, Washington, DC, April 1988, Pt. 3, pp. 1289–1293.

[6]Bogdanovich, A. E., and Yushanov, S. P., "Analysis of the Buckling of Cylindrical Shells with a Random Field of Initial Imperfections, Under Axial Dynamic Compression," *Mechanics of Composite Materials*, Vol. 17, No. 5, (English translation) 1981, pp. 552–560.

[7]Bogdanovich, A. E., and Yushanov, S. P., "Computing the Reliability of Anisotropic Shells from Probability of Infrequent Excursions of a Random Vector Field Beyond the Limiting Surface," *Mechanics of Composite Materials*, Vol. 19, No. 1, (English translation) 1983, pp. 67–75.

[8]Yushanov, S. P., and Bogdanovich, A. E. "Method of Computing the Reliability of Imperfect Laminar Cylindrical Shells with Allowance for Scatter in the Strength Characteristics of Composite Materials," *Mechanics of Composite Materials*, Vol. 22, No. 6, (English translation) 1986, pp. 725–730.

[9]Agarwal, B. D., and Broutman, L. J., *Analysis and Performance of Fiber Composites*, Wiley, New York, 1980, Chap. 4, 5.

[10]Jones, B. H., "Determination of Design Allowables for Composite Materials," *Composite Materials: Testing and Design*, ASTM Special Tech. Pub. 460, American Society for Testing and Materials, Philadelphia, PA, 1969, pp. 307–320.

[11]Clements, L. L., and Chiao, T. T., "Engineering Design Data for an Organic Fiber/Epoxy Composite," *Composites*, Vol. 8, No. 2, 1977, pp. 87–92.

[12]Lantz, R. B., and Baldridge, K. G., "Angle-Plied Boron/Epoxy Test Methods—A Comparison of Beam-Tension and Axial Tension Coupon Testing," *Composite Materials: Testing and Design*, ASTM Special Tech. Pub. 460, American Society for Testing and Materials, 1969, pp. 94–107.

[13]Staab, G. H., and Gilat A., "Behavior of Angle-Ply Glass/Epoxy Laminates under Tensile Loading at Quasi-Static and High Rates," *Proceedings of the American Society for Composites, Seventh Technical Conference*, Technomic, Westport, CT, 1992, pp. 1041–1050.